

Fabrication of Polymeric Hollow Spheres Having Macropores by a Quenching and Sublimation Process

Sang Hyuk Im and O Ok Park*

Department of Chemical & Biomolecular Engineering, Korea Advanced Institute of Science and Technology,
373-1 Guseong-Dong, Yuseong-Gu, Daejeon 305-701, Korea

Moo Hyun Kwon

Department of Chemical Engineering, Woosuk University, 490 Hujung-ri, Samrae-eup, Wanju-gun, Jeonbuk 656-701, Korea

Received Aug. 14, 2003; Revised Oct. 4, 2003

Abstract: We fabricated polymeric hollow spheres having macropores, which combine the advantageous properties of porous materials and hollow spheres. To fabricate such spheres, a polystyrene/methylmethacrylate solution was dispersed in water by vigorously stirring and then the suspension was quenched using liquid nitrogen. Water and methyl methacrylate present in the quenched suspension were readily sublimated by freeze-drying. Conclusively, the hollow-sphere structure and the macropores of its shell were created by the processes of liquid nitrogen-quenching and sublimation of methyl methacrylate domains within the shell, respectively.

Keywords: hollow spheres, macropores, freeze-drying, porous materials.

Introduction

Porous materials¹⁻⁸ have attracted much attention because of their unique advantageous properties such as high surface-to-volume ratio and low dielectric constant. These properties have been exploited in applications such as membranes and catalytic supporting materials.^{9,10} To date, most microporous materials have been made from inorganic materials. Recently, however, microporous materials based on organic polymers have been intensively studied as candidate materials for components of microelectronic devices.^{11,12} Hollow microspheres¹³⁻¹⁸ have generated particular interest because of their potential applications such as low-density capsules for controlled release of drugs, dyes, and inks, development of artificial cells, protection proteins, enzymes and DNA, as well as catalyst. Here we describe the preparation of polymeric hollow spheres with macropores. These hollow particles combine the advantageous properties of porous materials with those of hollow spheres.

Experimental

When a room temperature droplet of polystyrene/methylmethacrylate (PS/MMA = 60:40 wt/wt%; M_w of PS =

100,000; Aldrich Chem. Co.) solution is dropped into liquid nitrogen, the liquid nitrogen boils vigorously generating a strong convective flow that causes the droplet to spin around and around on the surface of the liquid nitrogen. This spinning motion causes the droplet to maintain a spherical shape during freezing. Finally, the frozen particle settles into the liquid nitrogen (see Figure 1 for a schematic of the freezing process). The frozen structure is maintained provided the temperature is below the freezing point of the solvent.

Results and Discussion

In the experiments reported here, the shape of the quenched structure was maintained because the temperature of

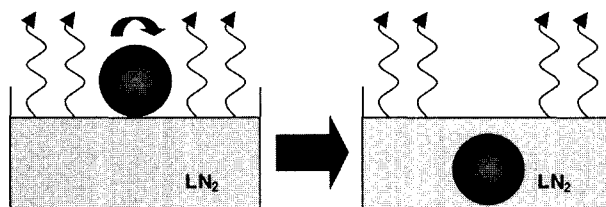


Figure 1. Schematic illustration of the process by which spherical particles form on immersion of a droplet of polymer solution in liquid nitrogen (LN₂). The polymer solution droplet spins on the surface of the LN₂ to form a spherical shape and then sinks into the LN₂.

*e-mail: ookpark@webmail.kaist.ac.kr

1598-5032/12/518-05 © 2003 Polymer Society of Korea

liquid nitrogen is much lower than the freezing point of MMA (-48°C). To remove the MMA from the frozen particle by sublimation, the particle was placed under vacuum for 1 day while maintaining the temperature as low as possible. During sublimation the temperature should ideally be kept below -48°C; however, in the present experiments the temperature increased at a rate of approximately 30°C/hr from -196 to 25°C due to shortcomings of the experimental setup. This problem did not seriously affect the experimental results because MMA sublimates enough fast before melting. Inspection of the structure after freeze-drying revealed that the spherical structure produced by the freezing process was

maintained during freeze-drying. The spherical shape of the freeze-dried particle indicates that the MMA solvent sublimated rather than melted during the freeze drying process, because if MMA had melted it would have readily dissolved the PS and consequently destroyed the spherical shape.

Figure 2(a) shows a cross-sectional scanning electron microscopy (SEM) image of the resulting sphere. From this image, it is clear that the interior of the sphere is empty. MMA can easily penetrate through spaces among polymer chains and disentangle and consequently expand the polymer occupying volume because MMA is a good solvent. When the PS/MMA solution droplet is dropped into liquid nitro-

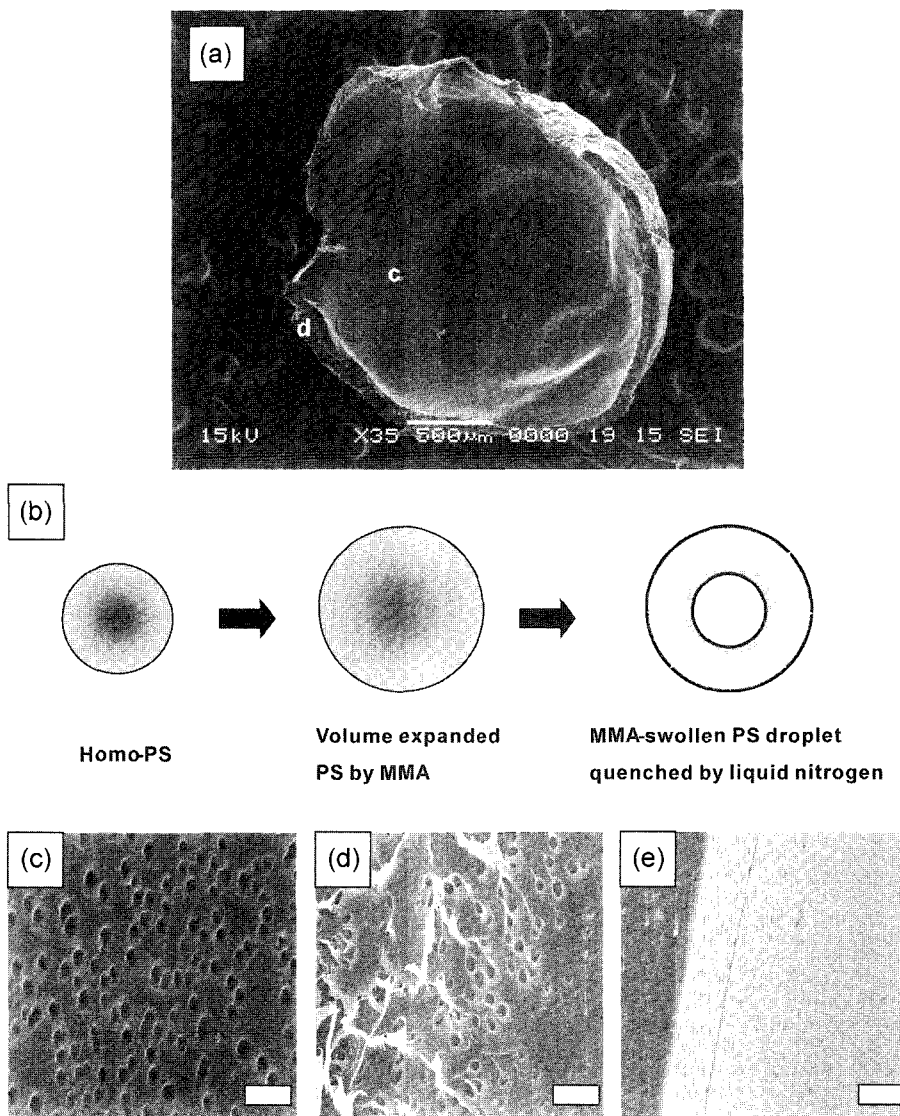


Figure 2. SEM images of a sphere with macropores obtained from quenching followed by freeze-drying of the solvent. (a) SEM cross-sectional image of a sphere. (b) Schematic illustration of the generation of a hollow sphere. First, PS is dissolved in MMA, expanding its volume. Then, the PS/MMA solution droplet is quenched from its surface. Finally, a hollow sphere is obtained due to the vitrification and contraction of PS. (c), (d), (e) SEM images of the inner wall-surface, the cross-section, and the outer wall-surface of the shell of the resulting sphere, respectively. Scale bars, 500 μm (a), 10 μm (c), (d), (e).

gen, this droplet begins to freeze from its surface, leading to vitrification of the polymer (PS) because the corresponding temperature is below the glass transition temperature ($T_g = 100^\circ\text{C}$) of PS. Accordingly, PS is solidified from the surface of the corresponding sphere and is contracted again toward the solidified wall (shell) as schematically shown in Figure 2(b). Therefore a hollow sphere is obtained.

Figures 2(c), (d), and (e) show three SEM images of the hollow sphere: the inner surface of the shell, a cross-section of the shell, and the outer surface of the shell. All regions show macropores ($1\sim 4\ \mu\text{m}$), which correspond to the volumes occupied by MMA in the original frozen structure. In addition, the spherical shape of the macropores indicates that MMA is frozen into spheres within the PS matrix, which is the most stable form from the viewpoint of surface energy. The pores of the outer shell-surface (Figure 2(e)) are smaller than those of the cross-section and the inner shell-surface (Figures 2(c) and (d)) because the outer shell-surface is preferentially frozen, which cause the morphology of the outer

shell to be quenched readily and the time it takes for MMA to freeze increases on going from the outer shell-region to the inner shell-region. Accordingly, the MMA near the inner surface of the shell aggregates into larger domains. Figure 2(d) clearly shows that the pores are isolated from each other (i.e., they are closed pores rather than open pores).

In addition to the millimeter-sized particles described above, we also successfully fabricated micron-sized hollow spheres with sub-micropores. Polymeric solution droplets with sizes on the order of micrometers were obtained by using a PS/MMA solution (0.5 mL) dispersed in water (4 mL) by vigorous stirring. In the resulting emulsion, the hydrophobic polymer solution forms spherical shapes in water to minimize its surface energy.

The suspension of PS/MMA solution dispersed in water was then dropped into liquid nitrogen in order to quench the structure and morphology. The quenched suspension was then immediately placed under vacuum for 1 day while maintaining the temperature as low as possible.

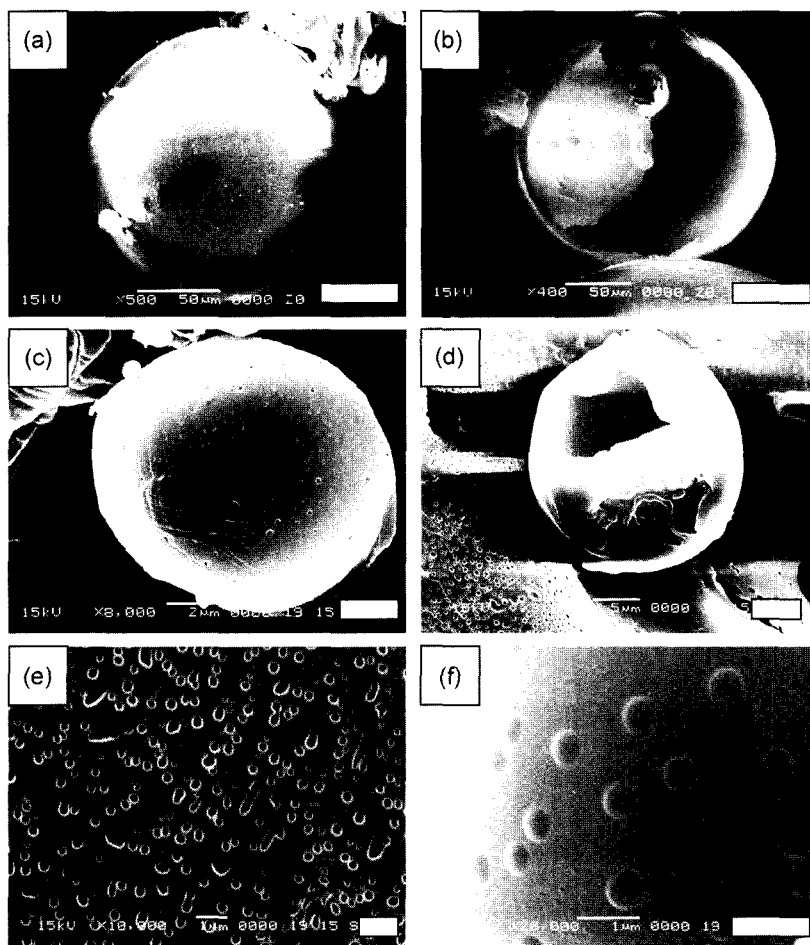


Figure 3 SEM images of micron-sized hollow spheres with macropores. (a), (c) SEM images of the resulting spheres whose diameters are approximately 150 and 10 μm , respectively. (b), (d) SEM images of broken spheres. (e), (f) SEM images of the inner wall-surface and the outer wall-surface of the shell of the broken sphere, respectively. Scale bars, 50 μm (a), (b), 2 μm (c), 5 μm (d), and 1 μm (e), (f).

SEM images of the resulting structures and morphologies are shown in Figure 3. Figures 3(a) and (c) show that the resulting structures are spherical in shape and have dimensions on the order of micrometers (10~150 μm). In addition, it is clear from these images that the outer surfaces of the particles are covered in numerous pores. Figures 3(b) and (d) show broken structures with sizes similar to those of the particles shown in Figures 3(a) and (c), respectively. The images of the broken particles make it clear that the particles are hollow. This hollow spherical structure forms by the mechanism described above. Figures 3(e) and (f) show magnified SEM images of the outer and inner surfaces of the shell of a broken particle, respectively. These images show that all of the regions have closed spherical pores whose sizes are sub-micrometer.

From a thermodynamic viewpoint, the condition for miscibility can be expressed as:¹⁹

$$\Delta G_{\text{mix}} = \Delta H_{\text{mix}} - T\Delta S_{\text{mix}} < 0$$

where ΔG_{mix} is the free energy of mixing, ΔH_{mix} is the enthalpy of mixing and ΔS_{mix} is the entropy of mixing. It can be stated that $\Delta G_{\text{mix}} < 0$ is a necessary but not sufficient condition for miscibility. Generally, the phase diagram of polymer-solvent mixtures is similar to that shown in Figure 4. In a PS/MMA mixture, PS and MMA are miscible and form a single phase at room temperature but are immiscible and separate into two phases at low temperatures (-196°C). The separation into two phases at low temperature occurs because in this regime the entropy term is small and consequently ΔG_{mix} becomes positive. In addition, when the PS/MMA mixture is quenched in liquid nitrogen, the MMA undergoes nucleation and growth. This leads to a sea-island

(PS phase-MMA phase) morphology in which the domain size of the islands (MMA) is related to the quenching rate because the quenching rate influences the growth time of the island phase. The suspending time required to completely freeze a sphere increases considerably with increasing sphere volume because the thermal conductivity of PS is very low; hence, the growth time of the island phase differs considerably between the micron-sized and millimeter-sized spheres. As a result, the size of the pores in the micron-sized hollow spheres (Figure 3) is smaller than that in the millimeter-sized hollow spheres (Figure 2). Moreover, it is well known that the morphology of the hollow sphere (e.g., sea-island vs. co-continuous) can be easily controlled by changing the quenching rate and the concentration of the polymer solution. This creates the possibility of preparing hollow spheres with a morphology suited to a particular application.

Conclusions

We successfully fabricated polymeric hollow spheres with macropores, which can be used in drug delivery systems, catalytic supporting materials, and so on. For drug delivery systems in a particular, the present work could be extended to create hollow spheres with macropores based on biocompatible and biodegradable polymers such as poly(lactide), poly(glycolide), and poly(lactide-co-glycolide) instead of PS.^{20,21}

Acknowledgements. The authors are grateful to the Center for Advanced Functional Polymers, which is supported by KOSEF. This work was also partially supported by the Brain Korea 21 Project.

References

- (1) M. Antonietti, B. Berton, C. Goltner, and H.-P. Hentze, *Adv. Mater.*, **10**, 154 (1998).
- (2) Y. Lu, H. Fan, A. Stump, T. L. Ward, T. Rieker, and C. J. Brinker, *Nature*, **398**, 223 (1999).
- (3) S. D. Sims, D. Walsh, and S. Mann, *Adv. Mater.*, **10**, 151 (1998).
- (4) D. A. Edwards, J. Hanes, G. Caponetti, J. Hrkach, A. Ben-Jebria, M. L. Eskew, J. Mintzes, D. Deaver, N. Lotan, and R. Langer, *Science*, **276**, 1868 (1997).
- (5) B. T. Kim, K. Song, and S. S. Kim, *Macromol. Res.*, **10**, 127 (2002).
- (6) S. C. Kim and B.Y. Lim, *Macromol. Res.*, **11**, 163 (2003).
- (7) J. S. Choi, B. C. Chun, and S. J. Lee, *Macromol. Res.*, **11**, 104 (2003).
- (8) J. H. Kim, J. E. Yoo, and C. K. Kim, *Macromol. Res.*, **10**, 209 (2002).
- (9) Y. Sakamoto, M. Kaneda, O. Terasaki, D. Y. Zhao, J. M. Kim, G. Stucky, H. J. Shin, and R. Ryoo, *Nature*, **408**, 449 (2000).
- (10) K. Sujatha and K. S. Kamalesh, *Ind. Eng. Chem. Res.*, **32**,

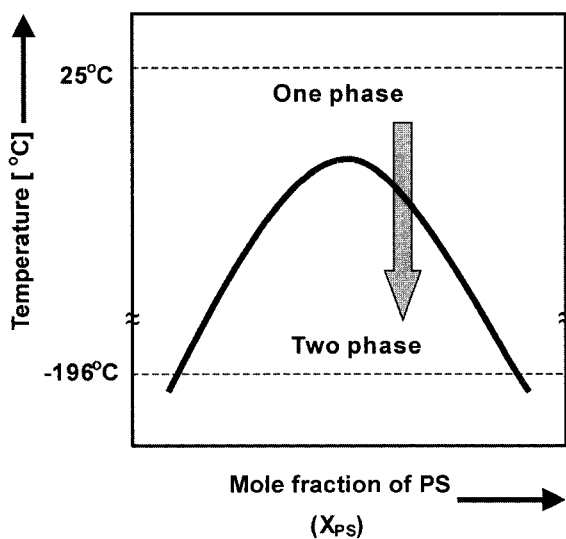


Figure 4 Typical phase diagram of PS/MMA mixture with mole fraction of PS (X_{ps}) versus temperature.

- 674 (1993).
- (11) K. R. Carter, J. L. Hedrick, R. Richter, P. T. Furuta, D. Mecerreyes, and R. Jerome, *Mat. Res. Soc. Symp. Proc.*, **431**, 487 (1996).
- (12) J. L. Hedrick, S. Srinivasan, R. D. Miller, D. Y. Shih, Y. -H. Liao, J. G. Hilborn, C. J. G. Plummer, and A. D. Martina, *Mat. Res. Soc. Symp. Proc.*, **431**, 511 (1996).
- (13) E. Muthusamy, D. Walsh, and S. Mann, *Adv. Mater.*, **14**, 969 (2002).
- (14) F. Iskandar, Mikrajuddin, and K. Okuyama, *Nano Lett.*, **2**, 389 (2002).
- (15) D. Wang and F. Caruso, *Chem. Mater.*, **14**, 1909 (2002).
- (16) M. S. Wong, J. N. Cha, K. -S. Choi, T. J. Deming, and G. D. Stucky, *Nano Lett.*, **2**, 583 (2002).
- (17) J. W. Kim, Y. G. Joe, and K. D. Suh, *Colloid Polym. Sci.*, **277**, 252 (1999).
- (18) D. L. Wilcox and M. Berg, *Mater. Res. Soc. Symp. Proc.*, **372**, 3 (1995).
- (19) U. W. Gedde, in *Polymer Physics*, Chapman & Hall, UK, 1995, pp 55-75.
- (20) R. T. Bartus *et al.*, *Science*, **281**, 1161 (1998).
- (21) R. A. Jain, *Biomaterials*, **21**, 2475 (2000).